Optical Pumping of Rubidium Atoms

Javier M. G. Duarte* and Sara L. Campbell†
Massachusetts Institute of Technology, MA 02142
(Dated: April 30, 2009)

We utilize circularly polarized light to 'optically pump' ground state natural rubidium isotopes into a nonthermal distribution in order to measure Zeeman splitting in the geomagnetic field. The signal, a variation in the opacity of the rubidium vapor induced by depolarizing RF photons, is detected with a photodiode. Helmholtz coils in three directions control the magnetic field and allow for two methods (varying frequency of RF photons or varying magnetic field) of determining the Landé g-factor for ^{87}Rb, $g_{87} = 0.495 \pm 0.003$, the Bohr magneton $\mu_B = (9.42 \pm 0.08) \times 10^{-24}$ J/T, and the ambient magnetic field $B_Z = 190 \pm 2$ mG (where we assume $g_{85} = 1/3$). In addition, the repolarization time constant is measured as a function of temperature and relative light intensity.

I. INTRODUCTION AND MOTIVATION

Alfred Kastler developed the technique, which he coined *optical pumping*, in the 1950s as way of altering atomic populations to form nonthermal distributions. The essential idea is that we pump and 'trap' atoms into a magnetic substate with the most polarization along the direction of an ambient magnetic field using specific incident light. When the magnetic substate energy levels are known, this polarized state allows for the measurement of weak magnetic fields (such as the earth's) with accuracy on the order of the substate spacing.

In this experiment, we apply this technique to measure the Lande g-factor for ^{87}Rb, the Bohr magneton, and the ambient magnetic field. We also discuss repolarization from a rapid 'flipping' of the magnetic field.

II. THEORY

A. Zeeman States

A single-electron atom placed in a uniform external magnetic field $\boldsymbol{B}$ experiences a perturbation to its Hamiltonian

$$\mathscr{H}' = -\frac{e}{2m}(\boldsymbol{L} + 2\boldsymbol{S}) \cdot \boldsymbol{B}. \tag{1}$$

where there are three separate contributions to the total atomic angular momentum: $\boldsymbol{I}$ the nuclear angular momentum, $\boldsymbol{L}$ the orbital angular momentum, and S the spin of the electron. Then $\boldsymbol{J} = \boldsymbol{L} + \boldsymbol{S}$ is the total electron angular momentum, and $\boldsymbol{F} = \boldsymbol{J} + \boldsymbol{I}$ is the total atomic angular momentum. In the weak-field limit, when fine structure is the dominant correction, we may simply take

$$\mathscr{H}' = -\boldsymbol{m}\boldsymbol{u}_f \cdot \boldsymbol{B} = g_f \frac{e}{2m}(\boldsymbol{F} \cdot \boldsymbol{B}), \tag{2}$$

where g_f is the Landé g-factor, which depends on the eigenvalues of the angular momentum operators in each state.

From 2, we see we are concerned with the projection of $\boldsymbol{F}$ in the direction of the magnetic field, which we may define as the z-direction. The eigenvalues are given by $\boldsymbol{F}^2 = f(f+1)\hbar^2$ and $F_z = m_f\hbar$. The eigenvalue m_f characterizes the magnetic substate and can range from $-f, -f+1, ..., +f$, while f can likewise range from $|j-i|, ..., j+i-1, j+i$

In our experiment, rubidium-87 and rubidium-85 have nuclear spin eigenvalues $i = 5/2$ and $i = 3/2$, respectively and we restrict ourselves to the ground state only ($s = 1/2, l = 0$ and thus $j = 1/2$). Therefore f can take on the values {2, 3} for ^{85}Rb and {1, 2} for ^{87}Rb.

$$g_f \simeq g_j \frac{f(f+1+j(j+1)-i(i+1)}{2f(f+1)}, \tag{3}$$

and g_J depends on the eigenvalue of $\boldsymbol{J}$ and evaluates to 2 for $J = 1/2$. Then, $g_f = 1/3$ for ^{85}Rb and $g_f = 1/2$ for ^{87}Rb (referred to as g_{85} and g_{87} herein after. Finally, from first-order perturbation theory, the correction to the hydrogenic energy eigenvalue may be written as,

$$E = E_0 + g_f m_f \mu_B |\boldsymbol{B}| \tag{4}$$

B. Optical Pumping

In this experiment, several different types of transitions and *selection rules* are involved in the optical pumping process. A *selection rule* specifies which transitions have negligible rates [1].

We proceed by irradiating the vapor with circularly polarized optical photons tuned to the transition $5^2S_{1/2} \rightarrow 5^2P_{1/2}$ (levels of varyling l). Since the incident photons have angular momentum $+\hbar$, the absorption must proceed with $\Delta m_f = 1$. Spontaneous emission, however, occurs rapidly ($\sim 10^{-8}$ s) with $\Delta m_f = 0, \pm 1$. The result is that once at atom reaches the $m_f = +f$ state of the 5S level, it is 'stuck.' Thus, the populations of atoms are 'pumped' toward the 5S state with the highest value of m_f.

*Electronic address: woodson@mit.edu
†Electronic address: campsoup@mit.edu

To actually measure differences between the Zeeman levels, we can do two things: (1) flood the vapor with radio frequency (RF) photons of the requisite resonant frequency to induce magnetic dipole transitions or (2) change the magnetic field s, we either flood the vapor with radio frequency (RF) photons of the requisite resonant frequency to induce magnetic dipole transitions or we change the magnetic field. These RF photons restore the populations to their thermal distribution so that the vapor can once again absorb the circularly polarized optical photons. Experimentally, we see this as an increase in opacity.

Finally, collisional deopolarization, which causes transitions between magnetic substates, limits this procedure.

C. Depolarization and Relaxation

The population of the $m_f = +f$ ground state, denoted by n, and the total population of the other grount state, denoted by N, are governed by the coupled linear first-order differential equations

$$\frac{dn}{dt} = -nW_\mathrm{d} + NW_\mathrm{u}, \frac{dN}{dt} = +nW_\mathrm{d} - NW_\mathrm{u} \qquad (5)$$

Here W_d (W_u) is the probability per unit time of downward (upward) transitons. If n_0 and N_0 represent the population at $t = 0$, then we can integrate and solve for the transmitted intensity as a function of the number of excess atoms in the $m_f = +f$ ground state

$$I = I_0 + \alpha(n - n_0) = I_0 + \alpha C(1 - e^{-t/\tau}), \quad \text{where } C = \frac{N_0 W_\mathrm{u} - n_0 W_\mathrm{d}}{W_\mathrm{u} + W_\mathrm{d}} \qquad (6)$$

and α is a constant.

III. EXPERIMENTAL DESIGN

A. Apparatus

Figure 1 shows a schematic diagram of the experimental apparatus. A rubidium vapor lamp provides D1 photons for the transition between $5^2\mathrm{S}_{1/2} \rightarrow 5^2\mathrm{P}_{1/2}$. The line is sufficiently Doppler broadened to allow for transitions between all magnetic substates. A linear polarizer and quarter-wave plate transmit only light with one sense of cirular polarization. The light is then collimated with a lense and incident on a sealed plexiglass cell contianing the rubidium. Forced hot air is blown into the cell from a heater beneath the table in order to vaporize the rubidium (melting point 38.5 ^{o}C). This cell also contains neon gas as buffer to reduce the rate of collisional depolarization. After the photons pass through the cell, they are focused by another lens on to a solid-state photodiode, which measures the intensity that we then display on an oscilloscope.

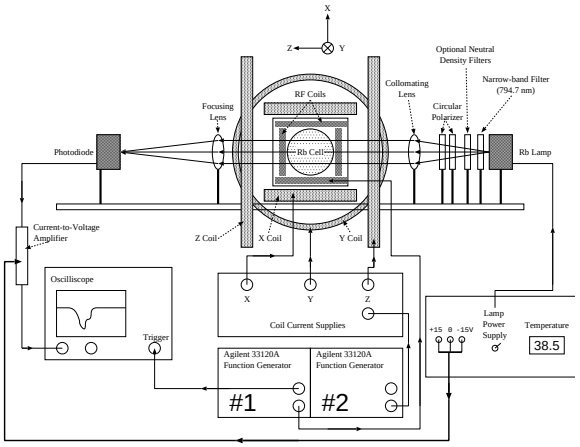

FIG. 1: The experimental setup. Taken from [2]

Three mutually perpendicular Helmholtz coils produce a highly uniform magnetic field over an extended region near their gometrical center given by

$$B = \frac{8\mu_0 NI}{\sqrt{125}R}, \qquad (7)$$

where I is the current through the coils in Amperes, N is the number of turns and $\mu_0 = 4\pi \times 10^{-3}$ G m A^{-1}. Note that the z-axis is defined as parallel to the 'beam' axis of the experiment.

We carried out two distinct types of experiments using the apparatus described above. Experiment 1 consisted of observing the depolarization of the rubidium atoms by RF photons. In experiment 2, we looked at the depolarization due to the magnetic substates suddenly becoming degenerate at zero magnetic field.

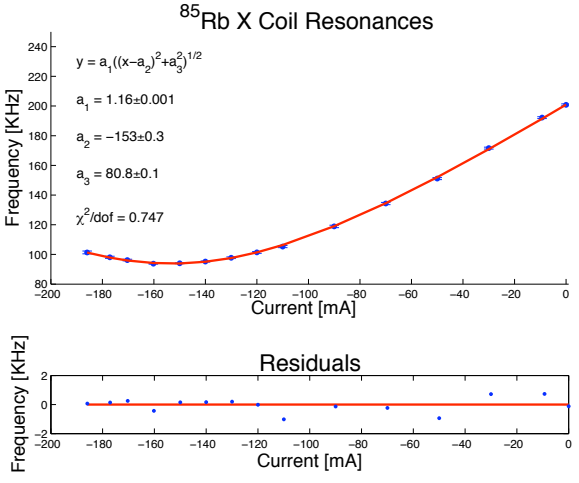

FIG. 2: Hyperbolic fit to the peak locations versus current for the x-axis coil data.

IV. DATA AND ERROR ANALYSIS

The data analysis was carried out in MATLAB using fitting scripts provided by the Junior Lab staff.

A. Determination of Zeeman parameters

We used two different methods to obtain measurements of the Zeeman spliting of rubidium and the ambient magnetic field. In method 1, we kept the Helmholtz current (magnetic field) constant and varied RF at each data point. In method 2, we kept the RF constant and swept through the Helmholtz current at each data point. Thus method 1 corresponds to data points in "current space," whereas method 2 involved looking in "frequency space."

1. *Constant Magnetic field, Varying RF*

We varied the x-axis Helmholtz coil current in steps from 0 mA to -185 mA. At each current, we swept the RF frequency from $\sim$ 0 to 300 kHz. We then repeated this procedure for the y and z-axis coils. We modeled the trace as a two-peak Lorentzian–corresponding to ^{85}Rb and ^{87}Rb–to find the peak locations.

From equation 4, we see that the frequency (i.e. peak location) is related to the components of the magnetic field:

$$\nu = \frac{g_f \mu_B}{h}\sqrt{B_x^2 + B_y^2 + B_z^2} \tag{8}$$

We performed a least-squares fit to the data for each isotope and direction. The result, for ^{85}Rb in the x-direction is shown in figure 2.

The minima of these hyperbola correspond to the zero magnetic field in that particular direction. From other parameters of the fit we can extract a measurement of $g_f/h\mu_B$. Assuming Planck's constant, we can only independetly measure two of the set $\{g_{85}, g_{87}, \mu_B\}$. We make the choice of taking $g_{85} = 1/3$ and thus we measure the other two parameters. Table I tabulates the results for our measurement of the magnetic field. The results are listed in table I.

2. *Constant RF, Varying Magnetic field*

Using the results of the previous fits we were able to 'buck' out the x and y components of the Earth's magnetic field. Then we applied a current ramp to z-axis coil and thus swept through B-field. We acquired traces at different frequency from 0 to 110 kHz. The data and $\chi^2_\nu = 3.26$ fit at 70 kHz, is displayed in figure 3. Again, we assume a Lorentzian lineshape and fit to an inverted five-peak distribution.

As labeled in the figure, the four smaller peaks correspond to the isotopes' resonances with the magnetic field. Equation 8 implies the resonance condition does not depend on the direction of the magnetic field–only the magnitude. Thus we see a symmetric distribution about $B = 0$. The larger peak in the center corresponds to the depolarization due to zero magnetic field (when all magnetic substates become degenerate and thus the Rb atoms may absorb light).

We plot the locations of the resonances against the frequency of the depolarizing photons in figure 4. Rearranging 8, setting $B_z = B - B_{z0}$, and combining the residual field in the x and y directions, $B_x^2 + B_y^2 = B_{xy}^2$, we recover the fit function listed in figure 4. Measurements of the ambient magnetic field B_{z0}

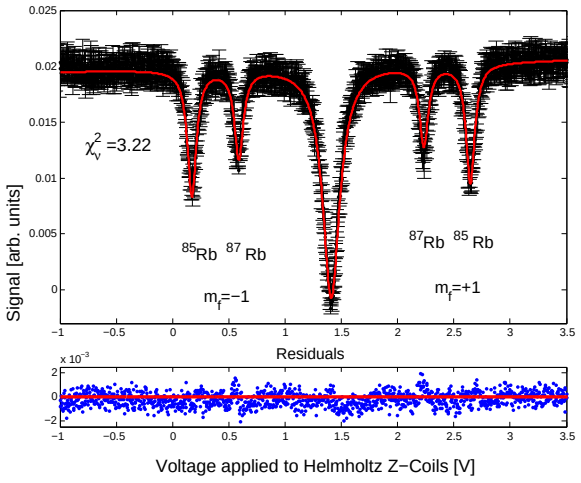

FIG. 3: Opacity changes due to sweeping z-axis magnetic field. Data was taken with depolarizing radio frequency set at 70 kHz.

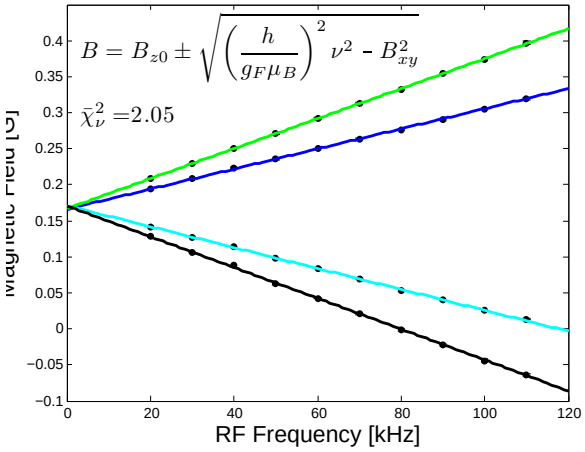

FIG. 4: Resonant magnetic field value plotted against the frequency of depolarizing photons.

	x-coils	y-coils	z-coils (1)	z-coils (2)	Accepted Hall	Accepted USGS
B_{x0}	380 ± 4	–	–	–	375 ± 13	503
B_{y0}	–	60.7 ± 0.6	–	–	58 ± 15	53
B_{z0}	–	–	189 ± 2	191 ± 2	191 ± 15	187
$\lvert B_0 \rvert$	429 ± 5				425 ± 19	539
φ [^{o}]	63.8 ± 0.2				63.3 ± 1.0	69.7
μ_B	9.29 ± 0.03	9.37 ± 0.08	9.51 ± 0.10	9.42 ± 0.08	9.27	
g_{87}	0.498 ± 0.002	0.492 ± 0.006	0.499 ± 0.002	0.495 ± 0.003	0.5	
$\%^{85}$Rb (x)	$52 \pm 8\%$	$54 \pm 1\%$	$51 \pm 5\%$	$57 \pm 4\%$	–	
$\%^{87}$Rb (x)	$48 \pm 8\%$	$46 \pm 1\%$	$42 \pm 5\%$	$43 \pm 3\%$	–	

TABLE I: Experimental results tabulated according to the method of measurement. The $x(y)$-coil indicates that we stepped through the current applied to $x(y)$-coil. This is also Method 1 for the z-coil. Method 2 for the z-coil indicates we swept the current applied to the z-coil, but stepped through frequency. All magnetic field measurements are quoted in milligauss. The Bohr magneton results are in units of 10^{-24} J/T.

B. Relaxation Effects

We first canceled the x and y-components of the geomagnetic field and then rapidly flipped the z-component of the magnetic field with a square wave input from the function generator. A DC offset was included to account for the z-component of the geomagnetic field.

1. *Intensity Dependence*

Essentially, the rubidium lamp (at fixed temperature) outputs a fixed total intentisty, which we label I_0. Since we cannot increase this intensity in a uniform manner, we vary the intensity by placing neutral density filters between the lamp and the focusing lens. We took the ratio of the intensity with the filter present to the intensity without the filter present, I/I_0 as our measure of relative intensity. Figure 5 displays the data on a log-log plot, the fit function, and the $\chi^2_\nu = 1.26$ least-squares fit. One feature is apparent: as the incident relative intensity I/I_0 approaches zero, the polarization time constant τ approaches $T_0 \equiv T + A/B$.

Qualitatively, when the magnetic field is flipped, the population in the $m_F = +1$ level switches with that of the $m_F = -1$ level. In the limit of zero intensity (no pumping), there will be a time when the inverted polarization of the atoms will also decay appreciably. The result is that the decay times τ converge against a characteristic 'spin relaxation' time T_0 [3]. As noted in figure 5, we measure $T_0 = 183.4 \pm 1.7$ ms.

2. *Temperature Dependence*

We applied the same square-wave 'flip' of the B-field, but stepped through temperature from $\sim$ 27 to 57 ^{o} C. To extract the repolarization time constant, we fit after the minimum to an inverted, decaying exponential. This extracted time constant was then plotted against temperature, as shown in figure 5. A functional relationship between this repolarization time and p the buffer gas pressure can be found in [4]:

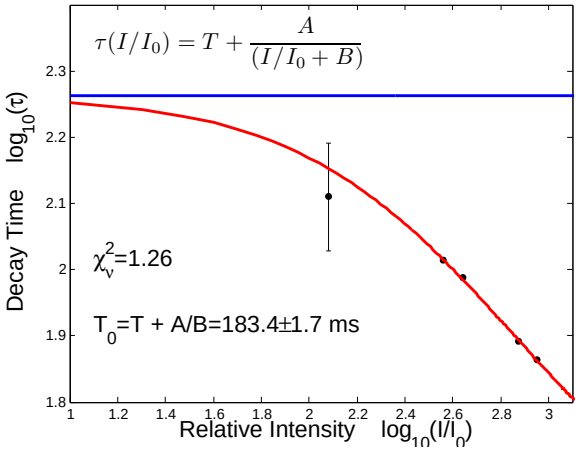

FIG. 5: Repolarization time constant against Intensity on a log-log plot.

$$\tau(p) \propto a_1\left(\frac{p}{a_2} + \frac{a_3}{p}\right), \tag{9}$$

From the ideal gas law, temperature is roughly proportional to pressure, so we fit directly to equation 9. The result of the $\chi^2_\nu = 1.39$ fit is plotted along with the data in 6.

V. DISCUSSION

In any analysis involving quantifying the magnetic field, including the determination of g_f, μ_B, and B_0, the error from the inhomogeneity of the magnetic field comprised nearly 100% of the total error. On the other hand, statistical and fitting errors dominated the measurements of relative abundance and the characteristic relaxation time. Temperature uncertainty also dominated the errors for repolarization measurements versus temperature measurements.

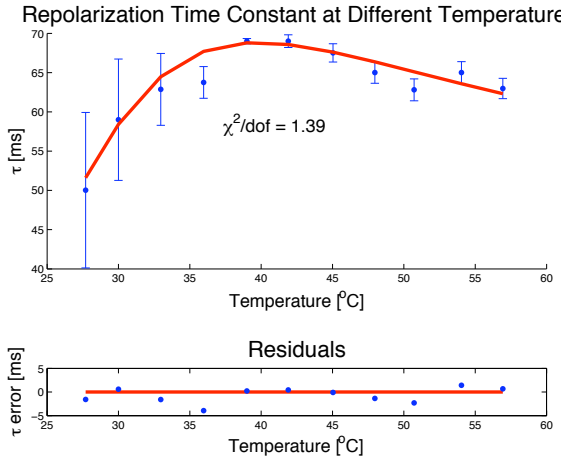

FIG. 6: Repolarization time constant plotted as a function of temperature.

The technique of optical pumping and controlled RF depolarization allowed us to investigate the magnetic parameters of the natural rubidium isotopes. Our magnetic parameter measurements are within 2σ of accepted values.

Acknowledgments

The author acknowledges Sara L. Campbell's equal partnership in the preparation and execution of this experiment. The author also thanks Professor Nergis Mavalvala, Stephen Jaditz, Regina Yopak, and Dr. Emily Edwards for their help and input.

[1] R. Eisberg et al. *Quantum Physics*. John Wiley and Sons, second edition, 1985.
[2] MIT Department of Physics. Optical pumping. Lab Guide, 2009.
[3] H. G. Dehmelt. Slow spin relaxation of optically polarized sodium atoms. *Phys. Rev.*, 105(5), 1956.
[4] W. Happer. Optical pumping. *Rev. Mod. Phys*, 44(2), 1972.